

Chapter 25

Structural, geomorphic, and depositional characteristics of contiguous and broken foreland basins: examples from the eastern flanks of the central Andes in Bolivia and NW Argentina

MANFRED R. STRECKER*, GEORGE E. HILLEY†, BODO BOOKHAGEN‡ and EDWARD R. SOBEL§

*Institut für Geowissenschaften, Universität Potsdam, Potsdam

†Department of Geological and Environmental Sciences, Stanford University, Stanford, USA

‡Geography Department, University of California, Santa Barbara, USA

§Institut für Geowissenschaften, Universität Potsdam, Potsdam, Germany

ABSTRACT

In this chapter, we contrast the elements of a typical, contiguous foreland basin system in the Bolivian Andes with the broken foreland farther south in northwestern Argentina. We illustrate differences in deposition and geomorphic shape that arise from the structural conditions to which these two systems are subjected. Generally, the principal elements of foreland-basin systems result mainly from accommodation space created by the flexural response of the crust to the topographic load of a fold-and-thrust belt. This leads to the formation of four distinct depozones: the wedge-top, foredeep, forebulge, and backbulge. In contrast, broken foreland basins are formed in areas where retroarc convergence is accommodated primarily along re-activated, high-angle structures. Rather than creating a broad area of consistently sloping mean topography, rock uplift along these structures is often disparate in space and time, leading to the formation of discrete ranges of limited along-strike extent that occur far inboard of the main topographic front of the orogen. The potentially high rock-uplift rates accommodated by steep, reactivated reverse faults favors isolation of the headwater basins of such systems from the downstream fluvial network, leading to sediment ponding behind the rising mountain ranges. In addition, the limited flexural response associated with short wavelength, laterally restricted topography may fail to create large amounts of accommodation space seen in the foredeep depozone that typifies foreland basin systems. Thus, instead of the generally continuous, laterally extensive foreland basin system associated with continental-scale crustal flexure, broken foreland basins, such as in the northwestern Argentine Andes, consist of a set of variably connected, laterally restricted depocenters. These evolve behind actively rising topography or small basins that form within the limited accommodation space created around individual uplifted mountain ranges. These types of depositional systems lack many of the elements that are typical of recent foreland basins, including well-developed foredeep, forebulge, and backbulge depositional systems. Instead of applying foreland basin models to broken foreland basin systems, it is important to view these systems in the context of their distinct structural, topographic, and geodynamic circumstances.

Keywords: contiguous foreland basin; broken foreland basin; fold and thrust belt; re-activated structures; central Andes

INTRODUCTION

The architecture of foreland basins and the thickness of their sedimentary fills are primarily determined by the creation of structurally controlled accommodation space associated with the lateral and vertical growth of fold-and-thrust belts (e.g., Dickinson, 1974; Jordan, 1981, 1995). Typically, four general tectonic/depositional domains characterize these environments, reflecting the interplay between shortening, crustal loading, climate, sediment production, and deposition (Fig. 25.1A) (e.g., DeCelles and Giles, 1996): (1) piggy-back basins, formed within and blind thrusting outboard of the extent of the fold-and-thrust belt define the boundaries of wedge-top basins, whose sediments are deposited within tectonically active portions of the orogen (e.g., Jordan, 1995; DeCelles and Giles, 1996); (2) flexural subsidence outboard of the fold-and-thrust belt provides space for foredeep sediments that thicken and coarsen towards the thrust wedge (e.g., Dickinson and Suczek, 1979; Schwab, 1986; DeCelles and Hertel, 1989; DeCelles and Giles, 1996); (3) the forebulge, a distal upwarped sector outboard of the foredeep, results from crustal-scale flexure (e.g., Jacobi, 1981; Karner and Watts, 1983; Quinlan and Beaumont, 1984; Crampton and Allen, 1995; Turcotte and Schubert, 2002); and (4) the backbulge basin is a second flexural basin created in the wake of the forebulge, defining a broad, low-energy depositional environment (e.g., DeCelles and Giles, 1996; Horton and DeCelles, 1997; DeCelles and Horton, 2003). As the fold-and-thrust belt advances into the foreland, these different tectonic and associated depositional domains also migrate systematically basinward, often leading to vertical

stacking of sediments created within these domains (e.g., DeCelles and Horton, 2003). The fold-and-thrust belt geometry approximates that of a self-similarly growing tectonic wedge that progressively entrains foreland-basin sediments by frontal accretion and motion along a detachment horizon, such as currently observed in the Subandean belt of Bolivia in the central Andes (e.g., Sempere et al., 1990; Kennan et al., 1995; Baby et al., 1997; Horton and DeCelles, 1997; McQuarrie, 2002; Uba et al., 2006).

This standard model successfully explains the primary features of both ancient and modern peripheral (*sensu* Dickinson, 1974) and retroarc foreland basins (e.g., Jordan, 1981, 1995; DeCelles and Giles, 1996). The model may be inappropriate for depositional basins in those orogens where contraction is accommodated by spatially disparate, diachronous, reverse-fault bounded basement uplifts, rather than a thin-skinned fold-and-thrust belt (e.g., Jordan and Allmendinger, 1986). Modern examples of such foreland basins include the Santa Barbara system of northwestern Argentina, adjacent to the Subandes fold-and-thrust belt, and the Sierras Pampeanas morphotectonic provinces farther south (Fig. 25.2; Stelzner, 1923; González-Bonorino, 1950; Allmendinger et al., 1983; Jordan and Allmendinger, 1986; Ramos et al., 2002). The Laramide foreland of the western United States (Steidtmann et al., 1983) may serve as an ancient analogue of such a basin system (Dickinson and Snyder, 1978; Jordan and Allmendinger, 1986). Although being related to a different geodynamic setting, the Tien Shan of Kyrgyzstan and China or the Qilian Shan uplifts north of the Tibetan Plateau comprise similar settings, where ongoing shortening excises and uplifts basement blocks in the

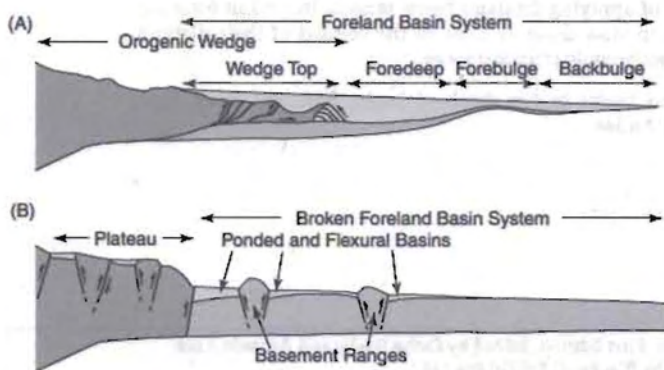


Fig. 25.1. Schematic (A) foreland and (B) broken foreland-basin system models. (A) Foreland basin systems consist of syn-deformational sediments deposited in the wedge-top, a foredeep depocenter created by flexure in front of an advancing fold-and-thrust belt, a forebulge depocenter that is located on the flexural bulge, and the backbulge basin located behind the flexural bulge (modified after DeCelles and Giles, 1996). (B) Broken foreland basins consist of sediment deposited within spatially limited flexural basins and sediment ponding behind rising topography.

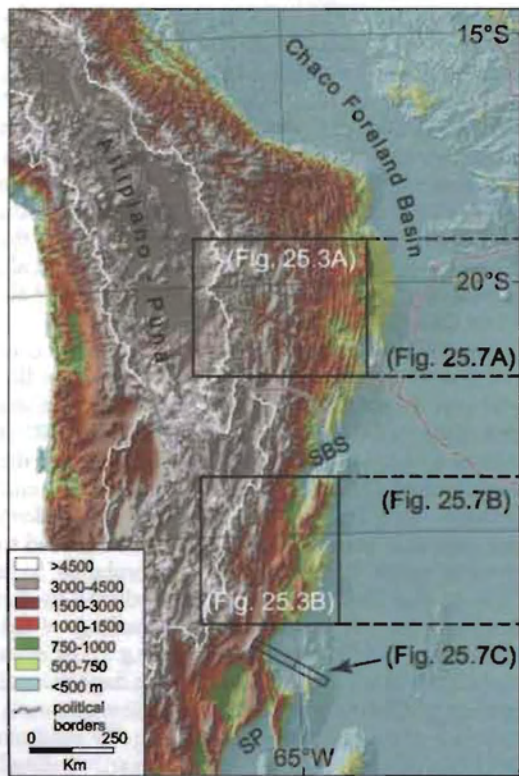


Fig. 25.2. Topography of the central Andes with elevations in m asl. Locations of longitudinal topographic swaths in Figures 25.4C and 25.4D are identical to the extents represented in Figures 25.3A and 25.3B, respectively. Mean topographic swaths (calculated laterally) used in the flexural models in Figures 25.7A, 25.7B, and 25.7C are also indicated. SBS and SP denote Santa Barbara and Sierras Pampeanas morphostructural provinces, respectively. Solid white line demarcates internally drained Altiplano-Puna plateau in the interior of the orogen.

foreland (e.g., Métivier et al., 1998; Sobel et al., 2003). This mode of foreland basin evolution eventually compartmentalizes a formerly contiguous sedimentary basin and often causes trends in rock uplift and sedimentation patterns that are not predicted by standard foreland basin models (e.g., Jordan and Allmendinger, 1986). This accommodation of deformation within basement ranges and the formation of a broken foreland may occur well inboard of the primary topographic margin of the orogen (e.g., Ramos et al., 2002; Strecker et al., 2009; Iaffa et al., 2011). Importantly, the uplift of such basement ranges leads to a different flexural

response than the one expected in typical foreland basin systems related to a growing orogenic wedge. Consequently, the evolution of associated depositional systems may be radically different compared to foreland basins adjacent to fold-and-thrust belts.

Here, we focus on the topographic, geomorphic, and depositional development of such broken foreland systems. We use the depositional system adjacent to the Puna Plateau and the Eastern Cordillera in northwestern Argentina to contrast the geodynamic conditions and development of this setting with the depositional system preserved in the Chaco foreland basin of Bolivia to the north (Fig. 25.2). Key differences between the structural development of the Bolivian and the northwestern Argentine Andes largely result from the differing pre-Cenozoic geologic history of these areas (e.g., Allmendinger et al., 1983; Kley et al., 2005), which has a profound impact on the flexural response of these two different areas to deformation, geomorphic development, and deposition in the surrounding basins.

RETROARC TOPOGRAPHY, DEFORMATION, AND DEPOSITION IN THE CENTRAL ANDES

Retroarc topography, deformation, and deposition in the central Andes between 15°S and 35°S (Fig. 25.2) results from convergence between the Nazca and South American plates and the geometry of the downgoing oceanic slab (e.g., Barazangi and Isacks, 1976; Bevis and Isacks, 1984). North of ~24°S, the subducting plate dips relatively steeply (~30°) beneath South America, while south of ~26°S, the slab shoals to a sub-horizontal geometry (e.g., Cahill and Isacks, 1992). There is a general correlation between this subduction geometry and the extent of high elevation in the Andean realm (Gephart, 1994). The internally drained Altiplano-Puna plateau spans southern Bolivia and northwestern Argentina between 15°S and 27°S and has an average elevation of 3.7 km (e.g., Allmendinger et al., 1997). This region comprises a contractional basin and range topography, characterized by isolated, sometimes coalesced sedimentary basins that host km-thick evaporitic and clastic sequences (e.g., Jordan and Alonso, 1987; Alonso et al., 1991; Vandervoort et al., 1995). These basins are bounded by high-angle reverse faults or volcanic edifices that either constitute the western margin of the plateau or further compartmentalize the basins in a transverse manner (Alonso et al.,

1984; Riller et al., 2001). To the east of the plateau and the Eastern Cordillera in Bolivia, a wedge-shaped ~250-km-wide fold-and-thrust belt defines the eastern border of the orogen. However, southward in northwestern Argentina, this fold-and-thrust belt vanishes and is replaced by a region of thick-skinned deformation within the Santa Barbara and Sierras Pampeanas ranges (e.g., Allmendinger et al., 1983; Mon and Salfity, 1995). The spatial extent of the fold-and-thrust belt in Bolivia correlates with thick Paleozoic units, in which a series of Silurian, Devonian, and Carboniferous detachment surfaces define the basal decollement of the orogenic wedge (e.g., Sempere et al., 1990; McQuarrie, 2002; Elger et al., 2005). However, approximately south of 24°S, these mechanically weak layers become significantly thinner and eventually disappear, and the thin-skinned style of deformation terminates (e.g., Allmendinger et al., 1983; Mon and Salfity, 1995; Cristallini et al., 1997; Kley and Monaldi, 2002). Instead, inverted normal faults and transfer structures related to the Cretaceous Salta Rift have often accommodated shortening during the Cenozoic Andean orogeny (Grier et al., 1991; Kley and Monaldi, 2002; Carrera et al., 2006; Hongn et al., 2007; Hain et al., 2011). In addition, the metamorphic fabrics generated during the early Paleozoic (Ordovician) Ocloyic orogeny follow the western margin of the broken foreland uplifts in the transition to the Puna Plateau and are inferred to have affected the spatial characteristics of contractile reactivation during Andean shortening (e.g., Mon and Hongn, 1991). The reactivated, inherited, extensional and contractional anisotropies have produced discrete ranges that occur both along the eastern flank of the plateau as well as far to the east of the plateau margin within the otherwise undeformed foreland, as might be expected from the mechanics of reactivation of pre-existing weak structures in the crust (Mon and Salfity, 1995; Hilley et al., 2005). This is virtually identical to inverted extensional structures in the Eastern Cordillera of Colombia (e.g., Mora et al., 2006; Parra et al., 2009) and bears resemblance to the pattern of reactivated structures in the North American Laramide province (Marshak et al., 2000). Thus, the pre-Andean paleogeography of northwestern Argentina has left an imprint on the manner in which Cenozoic shortening is accommodated, resulting in a broad zone of deformation without a well-defined, tectonically active orogenic front

and unsystematic lateral growth (e.g., Allmendinger et al., 1983; Grier et al., 1991; Mon and Hongn, 1991; Reynolds et al., 2000; Carrera et al., 2006; Ramos et al., 2006; Hongn et al., 2007; Hilley and Coutand, 2010). The broken foreland in Argentina therefore constitutes a morphotectonic province with spatially and temporally disparate range uplifts and intervening basins, a setting akin to the hydrologically isolated adjacent basins of the Altiplano-Puna in the orogen interior (Alonso et al., 1984, 1991; Jordan and Alonso, 1987; Kraemer et al., 1999; Carrapa et al., 2005).

The differences in deformation style in the central Andes have fundamentally impacted the fluvial and depositional system. Within, and to the east of the Bolivian fold-and-thrust belt, deposition occurs within a wedge top that transitions into the undeformed Chaco foredeep deposits to the east (Horton and DeCelles, 1997). These foredeep deposits thin towards the east and are inferred to thicken again to the east of the forebulge high (Horton and DeCelles, 1997), as predicted by the flexure incurred by topographic loading of the advancing fold-and-thrust belt (e.g., DeCelles and Giles, 1996). In stark contrast, the depositional system within northwestern Argentina generally consists of variably connected, partially separate depocenters, whose margins are primarily defined by basement uplift along crustal anisotropies. Unlike the foreland basin system within Bolivia or in the northernmost part of the Argentine Subandean province, this region lacks a deep and laterally extensive foredeep and only contains subdued back- and forebulge areas. For example, in the Santa Barbara system the foreland deposits have a thickness of approximately 3000 m (Cristallini et al., 1997; Bossi et al., 2001). In the transition to the Subandean ranges, sedimentary thickness increases (Reynolds et al., 2001) and reaches more than 7000 m in the Argentine and southern Bolivian sectors of the Subandean fold-and-thrust belt (Echavarria et al., 2003; Uba et al., 2006). The hydrologic connectivity of basins within this broken foreland has varied over geologic time. The generally arid to sub-humid basins virtually all show evidence of several transitions between internal and external drainage (Strecker et al., 1989, 2007, 2009; Mortimer et al., 2007), suggesting a complex relationship between tectonic movements, drainage adjustments, and climate (Starck and Anzótegui, 2001; Hilley and Strecker, 2005).

TOPOGRAPHIC AND GEOMORPHIC CHARACTERISTICS OF THE EASTERN ANDEAN MARGIN IN BOLIVIA AND NW ARGENTINA

The contrasting deformational style observed within Bolivia and northwestern Argentina is clearly revealed in the topography of these two areas. Deformation within the Bolivian fold-and-thrust belt is characterized by laterally continuous thrust faults that have surfaced from the mechanically weak decollement horizons. The along-strike continuity of thrust-fault geometry likely results from lateral homogeneity of the underlying strata (e.g., Allmendinger et al., 1983; Sempere et al., 1990; Hilley and Coutand, 2010), creating virtually uninterrupted ridges oriented perpendicular to the regional shortening direction (Figs. 25.2 and 25.3A). This pattern of topography can be most clearly seen by examining the variability of elevations between adjacent points. In Bolivia, elevations perpendicular to the shortening direction or along strike of the orogen are well correlated in space (over length scales of >50 km; Fig. 25.4A). Elevations parallel to the shortening direction or parallel to the topographic gradient are far less consistent. Thus, following a contour line in southern Bolivia allows one to move along the trend of the orogen over great distances, with interruptions only occurring in antecedent river valleys cutting through the topography. In addition, the mechanics of fold-and-thrust belt deformation favors a geometry in which the surface of the orogenic wedge thickens toward the back of the belt and tapers toward its front (e.g., Dahlen, 1984). Thus, while

these fold-and-thrust-fault related ridges form significant topographic variations along the direction of shortening, the mean topographic slope along ~300 km of the fold-and-thrust belt is quite consistent (Fig. 25.4C).

In contrast, within northwestern Argentina, elevations are much less consistent over long length scales as shortening is accommodated within discrete basement ranges. In these areas, elevations are typically correlated over distances of ~20 km in the direction perpendicular to convergence (Fig. 25.4B). The reverse-fault-bounded blocks are far more discontinuous than structures in the fold-and-thrust belt, resulting in the prevalence of structural gaps through which drainages may be routed (Trauth et al., 2000; Strecker and Marrett, 1999; Sobel et al., 2003). In addition, easterly moisture-bearing winds may penetrate along large valleys into the interior of the arid orogen during negative ENSO years (Strecker et al., 2007; Bookhagen and Strecker, 2008, 2010). Mean elevations profiled perpendicular to shortening show much greater variability and are characterized by the short wavelength topographic features extending into the foreland, which represent discrete uplifts along reactivated structures (Fig. 25.4D).

The geomorphic development of basins within the deforming portion of these areas reflects the different ways in which shortening is accommodated in the two different foreland types. In Bolivia, large, regional-scale drainages traverse the fold-and-thrust belt, and a trellis drainage pattern routes runoff between ridges (Fig. 25.5A). At the orogenic front, megafans store sediment supplied from the orogen and are transitional with braidplains farther

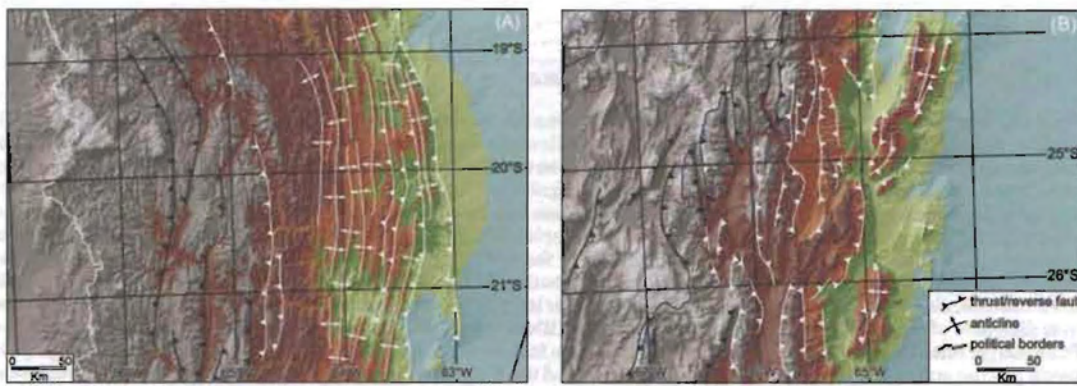


Fig. 25.3. Detailed topography and structures in the Subandean fold-and-thrust belt in Bolivia (A) and the associated Chaco foreland basin system. (B) Puna Plateau margin and Santa Barbara/Sierras Pampeanas morphostructural provinces.

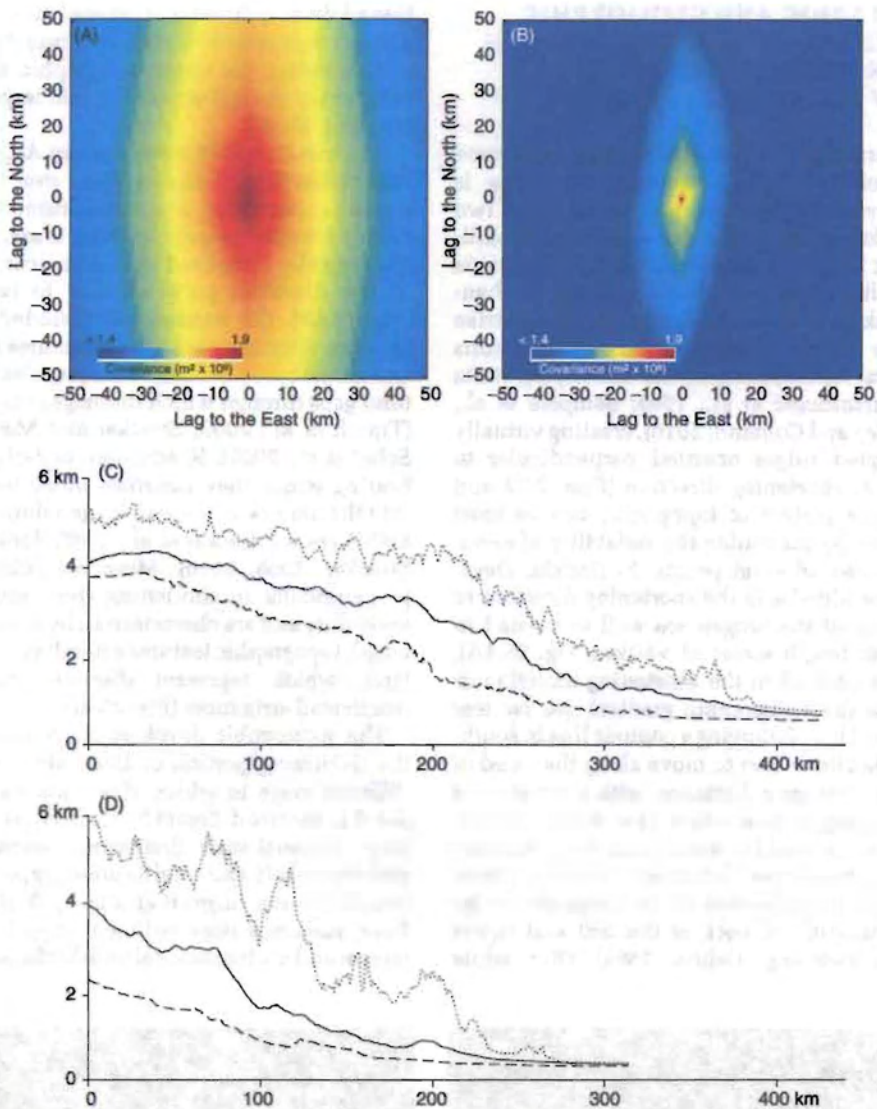


Fig. 25.4. Variograms of topography within (A) the Subandean fold-and-thrust belt, and (B) eastern Altiplano-Puna margin in northwestern Argentina, showing the spatial correlation of elevation as a function of directional lag distance. This correlation function was computed by comparing the correlation between the elevations of each pixel in the DEM and the corresponding pixel whose location is offset a specified direction and magnitude (directional lag distance). In areas where elevations are similar at large distances from one another, covariance values will be large. In addition, the diagrams show how elevations covary as a function of direction from a given point. For example, covariance between elevations that persist in a N-S direction relative to the E-W direction at larger distances are seen by the N-S elongation of large covariance values. The extent of the topography used to calculate variograms in (A) and (B) is identical to that shown in Figures 25.3A and 25.3B, respectively. In the Subandes, elevations are correlated in N-S direction over long (> 50-km) length scales, whereas topography is correlated over distances of only ~20 km in the broken foreland. This illustrates the discontinuous nature of the topography along the Puna margin relative to that observed within the Subandean fold-and-thrust belt. (C) and (D) show longitudinal topographic swath profiles across the Subandean fold-and-thrust belt and the Altiplano-Puna margin, respectively. Solid lines represent the mean topography, while dotted envelopes bounding the top and bottom of the profile denote the maximum and minimum topography within each swath, respectively.

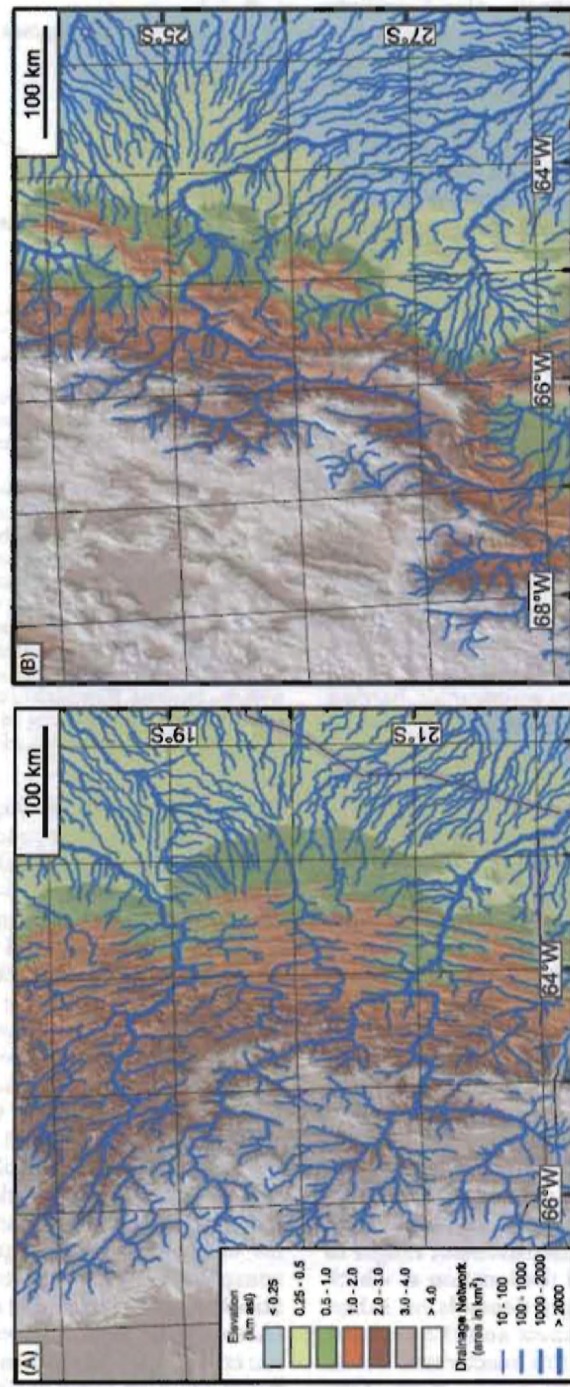


Fig. 25.5. (A) Drainage patterns in the Subandean fold-and-thrust belt and adjacent regions of southern Bolivia; and (B) drainage patterns in the broken foreland provinces and adjacent areas of northwestern Argentina. No drainage pattern for the internally drained Altiplano-Puna Plateau is shown.

east (Horton and DeCelles, 2001; Wilkinson et al., 2010). Megafan deposits also constitute older sedimentary rocks that were deposited beginning at 8 Ma, now forming an integral part of the deforming orogenic wedge (e.g., Uba et al., 2006, 2007). In contrast, in the region of the Santa Barbara and Sierras Pampeanas, several generations of transient basin fills were deposited and re-excavated in all of the intermontane basins that are near the headwaters of rivers currently draining the broken foreland basin system (Hilley and Strecker, 2005; Mortimer et al., 2007; Strecker et al., 2007). These sediments often onlap and are sometimes over-thrust by downstream basement ranges that accommodate convergence in this area (Bossi et al., 2001). The transient basin fills have typically formed where easterly moisture-bearing winds are prevented from reaching the basin headwaters by downwind basement ranges, which form efficient orographic barriers (Sobel and Strecker, 2003; Hilley and Strecker, 2005; Coutand et al., 2006; Strecker et al., 2007; Bookhagen and Strecker, 2008). Based on the results of analytical models (Sobel et al., 2003; Hilley and Strecker, 2005), the formation of internal drainage and sediment accumulation appears to be a threshold process in which active uplift of downstream topographic barriers steepens channels that traverse these ranges, while aggradation behind the uplifting range must keep pace with the rise of the channel bed as rock uplift occurs. Internal drainage is favored as rock uplift rates increase, and bedrock erodibility and/or precipitation decrease. In addition, in the case that channels traversing the bedrock range prior to its uplift are steep, external drainage is favored compared to a setting in which initial channel slopes are low (Fig. 25.6; Sobel et al., 2003). Conversely, low rock-uplift rates in the downstream basement ranges, a high degree of erodibility of exposed rock types, and pronounced rainfall gradients all promote incision, headward erosion, and basin capture. All of these processes are conducive to sustaining fluvial connectivity with the foreland (Hilley and Strecker, 2005).

In contrast to the along-strike consistency of deformation in the Bolivian fold-and-thrust belt, deformation within the basement ranges to the south is disparate and the location at which deformation occurs strongly depends on inherited crustal zones of weakness and the evolving topographic load above the reactivated faults (Bossi et al., 2001; Hilley et al., 2005; Kley et al., 2005; Mortimer et al., 2007; Iaffa et al.,

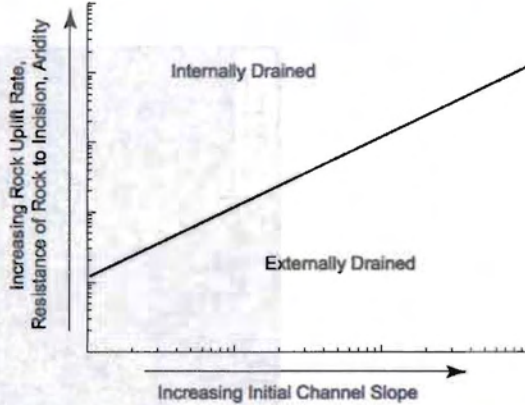


Fig. 25.6. Schematic depiction of the factors that control the threshold between internal and external drainage. The increasing values along the x-axis represent greater initial channel slopes prior to uplift of downrange topography, while the y-axis depicts the effect of increasing rock uplift rate, resistance of bedrock to fluvial incision, and/or aridity. The solid line shows the combinations of initial channel slope and rock uplift rate/erosional resistance/climate that are required to produce basins that are at the verge of internal drainage. Basins with conditions that plot above this line are expected to eventually become internally drained as uplift proceeds downstream, while those that plot below the threshold line will maintain a connection with the foreland. How each of these factors may be used to predict conditions resulting in internal drainage, is presented in Sobel et al. (2003) and Hilley and Strecker (2005).

2011). In addition, the high-angle contractional structures in this area produce larger amounts of uplift for a given increment of shortening than the low-angle thrusts in Bolivia. This may facilitate the rapid removal of cover sediments from atop the rising basement-cored mountain ranges, thus exposing lithologies resistant to erosion (e.g., Sobel and Strecker, 2003). Finally, owing to the atmospheric circulation patterns in this part of the Andes, the basement-cored ranges may concentrate moisture on their windward sides. For example, the eastern flanks of these basement ranges receive between 1.5 and 3 m/yr of rainfall, while the intermontane basins often receive < 0.3 m/yr (e.g., Bookhagen and Strecker, 2008). This leads to the aridification of the headwaters of basins in the lee of the rising topographic barrier. This may conspire to cause a transient (Hilley and Strecker, 2005; Strecker et al., 2009) or permanent (Alonso et al., 1991; Vandervoort et al., 1995; Horton et al., 2002) decrease in erosional power of the rivers draining these basins, reducing the likelihood of fluvial connection with the foreland.

The discontinuous nature of deformation within northwestern Argentina has produced spatially disparate and diachronous storage of sediments upstream of the uplifting ranges (Bossi and Palma, 1982; Strecker et al., 1989, 2009; Hilley and Strecker, 2005; Carrapa et al., 2009). Within basins flanking the margins of the Puna Plateau, conglomerates sourced from the Puna margin and ranges surrounding these basins are sometimes intercalated with lacustrine sediments as well as tephras that constrain the timing of deposition of these sediments. The disparate nature of the basin fills suggests that local conditions, such as rock uplift within the surrounding ranges, rock erodibility, microclimates surrounding the individual basement ranges, and/or differing basin geometries may play a larger role in controlling basin filling than regional factors, such as mesoscale climate changes that are correlated in space and time (Strecker et al., 2007).

At first sight, the short strike lengths of the faults bounding the uplifts in the broken foreland may be expected to aid the formation of an external drainage system as rivers would have to flow a shorter distance along strike in order to circumvent the growing inverted structures. Conversely, in the foreland fold-and-thrust belt extensive ridges parallel to the trend of the orogen should favor internal drainage conditions. However, rainfall and discharge amounts as well as the loci of maximum precipitation in the two morphotectonic provinces are very different and influence erosion processes in a fundamental way. Whereas precipitation is higher and much more focused in an elevation sector between 1500 and 2000 m along the orogenic wedge in the fold-and-thrust belt, it is more widely distributed in the broken foreland in northwestern Argentina (Bookhagen and Strecker, 2008). This influences erosional efficiency, an assessment which is supported by differing specific stream-power values in both regions (Bookhagen and Strecker, 2010). Specific stream power is generally higher in the regions to the north, where high erosion rates correlate with areas of high rainfall, high relief, and steep fluvial channels (Safran et al., 2005), whereas lower values characterize the broken foreland areas. This trend may be exacerbated during negative ENSO years, when a threefold increase in rainfall may occur (Bookhagen and Strecker, 2010). As the ENSO system has existed at least since the Pliocene (e.g., Wara et al., 2005), a protracted influence of the associated precipitation and erosion characteristics on landscape evolution and sedimentary

processes is to be expected. Thus, the combined effects of differences in climate and efficiency of erosion, as well as the contrasting nature of deformation between the fold-and-thrust belt and the broken foreland cause the topography and geomorphic development of the southern region to be far more discontinuous than the northern region.

DIFFERENTIAL FLEXURAL RESPONSE TO TOPOGRAPHIC LOADING ALONG THE CENTRAL ANDES

The development of foreland basin systems primarily results from the accommodation space created by crustal-scale flexure (e.g., Jordan, 1981). This crustal-scale flexure is caused largely by long-wavelength topographic loading within the orogen's interior, which is transmitted to the adjacent foreland through elastic stresses within the crust. In foreland basins, topographic loading within a wide fold-and-thrust belt can deform the crust at great distances from the orogenic front, leading to the formation of foredeep, forebulge, and backbulge accommodation zones. However, in broken foreland basins such as those discussed here, rock uplift within areas bounded by weak, reactivated structures may form steep mountain ranges restricted in both their along- and across-strike dimensions. Because the spatial extent and amount of accommodation space created by flexural loading scales with the wavelength of the load (e.g., Turcotte and Schubert, 2002), we might expect that these types of short-wavelength features create less accommodation space than their longer-wavelength counterparts.

Figure 25.7 illustrates a model of the flexural accommodation that might be caused by the modern mean topography across a typical longitudinal transect of the Bolivian fold-and-thrust belt (Fig. 25.7A) and the central Andean broken foreland (Fig. 25.7B). The flexure created by the topography that lies above baselevel is denoted by dashed lines for a the case of a stiff lithosphere (flexural rigidity, $D = 7 \times 10^{23}$ Nm; Horton and DeCelles, 1997) and by dotted lines for the case of a soft lithosphere ($D = 2 \times 10^{22}$ Nm). This flexural model is one-dimensional, where the out-of-plane extent of the mean topography is assumed to be large compared with the swath width. While this assumption is likely reasonable for the laterally continuous fold-and-thrust belt, the along-strike discontinuities of the broken foreland lead to an overestimation of the amount of accommodation space that is created by

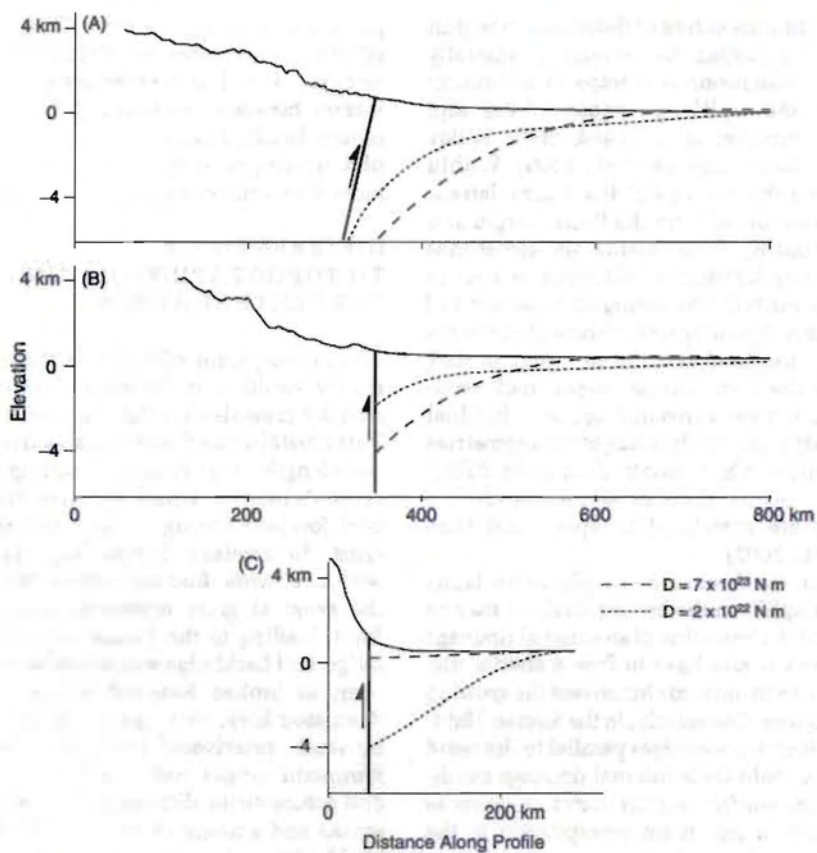


Fig. 25.7. Flexural accommodation response based on the observed mean topography along the (A) Subandean fold-and-thrust belt and associated foreland basin system, and (B) Puna margin and associated broken foreland basin system, and (C) across Sierra Aconquija at approximately 27° S lat. In A, B and C x axis corresponds to distance along profile and y axis corresponds to elevation of transects indicated in Fig. 25.2. We use the topography extracted from topographic swaths through these two transects (shown in Fig. 25.2A) with an implicit finite-difference scheme that calculates the deflection of the crust for a given mantle and crustal density (3300 kg/m^3 and 2700 kg/m^3 , respectively) and flexural rigidity ($Eh^3/(12(1-v^2))$, where E , h , and v are the Young's modulus, elastic thickness, and Poisson's ratio of the crust, respectively (Turcotte and Schubert, 2002). We assume $E=50 \text{ GPa}$, $h=49$ and 15 km , and $n=0.25$ for illustration), while fixing displacements and rotations at the right end of the model to zero. The left boundary was extended by a factor of two from the location shown, and a topographic load equal to that exerted at the left side of the profile was uniformly applied to the area. This insured that any isostatically uncompensated portion of the Puna-Altiplano plateaus' loads were transmitted into the foreland. The thin-plate flexure equation (with no end load) was solved using an implicit finite-difference scheme using the topographic load above base-level (defined by the elevation at the eastern ends of the mean profiles). The flexural rigidities that result from different assumed elastic thicknesses are $D=7 \times 10^{23} \text{ Nm}$ and $D=2 \times 10^{22} \text{ Nm}$. The mean topography is shown as a solid line in (A-C), while the calculated base of the sediments in the subsiding basins is shown as a dashed and dotted line for the stiff and soft crust scenarios, respectively. In the Subandes, flexural accommodation reaches farther into the foreland and is deeper than in the Santa Barbara and the Sierras Pampeanas systems, owing to the broad geometry of the fold-and-thrust belt.

flexural loading. Nonetheless, the two end-member models from the Andes shown here clearly illustrate the key differences in the creation of accommodation space in these two structural settings.

In the case of the Bolivian Subandes, the broad gently tapered fold-and-thrust belt creates a

topographic load that is transmitted far into the South American craton. Flexural subsidence adjacent to the fold-and-thrust belt forms accommodation space for the foredeep depozone, while uplift of the forebulge ~450 km from the front of the orogenic wedge creates an area where either material is

eroded or deposition is limited. Flexural subsidence within the backbulge basin may create some additional accommodation space for sediments, although deeper geodynamic processes such as mantle downwelling within the asthenospheric wedge may augment subsidence in this case (Mitrovica et al., 1989; DeCelles and Giles, 1996). As the lithosphere becomes less rigid, the foredeep becomes more restricted in its spatial extent as deflection of the basin bottom far from the topographic front reflects isostatic, rather than flexural compensation of the gently sloping topography.

In the case of the NW Argentine broken foreland basins, the flexural response is far more subdued for both rigidities investigated (Fig. 25.7B) due to the short-wavelength nature of the topography east of the plateau margin. The tapered load in Bolivia imparts a larger force over the wavelengths that are flexurally compensated than the more abrupt load of the steep Argentine margin. This leads to a foredeep that is more restricted in Argentina than in Bolivia. In addition, flexural subsidence may occur adjacent to individual basement ranges, such as that adjacent to Sierra Aconquija (Bossi et al., 2001; Cristallini et al., 2004; Fig. 25.7C) or immediately to the north along Cumbres Calchaquíes (de Urreiztieta, 1996). However, the spatial extent of the surrounding depocenters is limited relative to the foredeep (Fig. 25.7B). In the case of a stiff crust, little accommodation space is created by the topographic load of these features. The abrupt topographic feature can locally create accommodation space of up to ~4 km when the rigidity of the crust is low. Seismic reflection data from the Sierra Aconquija area suggest that Cenozoic sediments may reach a thickness of ~3.5 km adjacent to the range (Cristallini et al., 2004), suggesting that in these areas, crustal rigidity may in fact be low. Indeed, low elastic thickness values estimated for this region support this inference (Tassara et al., 2007). For such a weak crust, the principal pattern of accommodation space mimics that of the deformation. In the northwestern Argentine Andes, flexural accommodation may thus be spatially limited and discontinuous, and the location of basins may ultimately be controlled by the distribution of reactivated zones of crustal weakness (Hilley et al., 2005; Kley et al., 2005; Hongn et al., 2007; Hain et al., 2011). In addition, due to the link between crustal heterogeneities and their compressional reactivation, the evolution of the broken foreland is unsystematic, diachronous,

and may additionally depend on the local lithostatic stresses exerted by the neighboring range uplifts. The individual depocenters created by flexure may be connected to upstream basins formed by sediment ponding behind rising basement ranges and the downstream regional baselevel by a system of fluvial channels that traverse the broken foreland. However, a pronounced forebulge and backbulge is subdued in such settings, as deflection of the crust primarily results from isostatic compensation over long wavelengths, rather than the flexural compensation that produces uplift in the forebulge.

In the central Andes, it is likely that both the geometry of the topography and the rigidity of the lithosphere play an important role in controlling the creation of accommodation space. In general, in the Bolivian Andes, the Subandean fold-and-thrust belt is characterized by a continuously, and gently, tapered topography. Additionally, the fact that deformation here is accommodated along subhorizontal detachment horizons in the sedimentary basin suggests that crustal weaknesses may be less pronounced than farther south in Argentina. In contrast, the steep Andean front in Argentina is accompanied by basement uplifts suggesting that pre-existing reactivated structures weaken the crust. Both the differing topographic loading and the likely lower flexural rigidity of this sector of the Andes favors the creation of local accommodation space in a broken foreland setting, rather than a continuous foreland basin system as farther north in Bolivia.

CONCLUSION

The accommodation space within foreland basin systems that ultimately serves as a sediment depocenters is created primarily by the flexural response of the crust to the topographic load of a fold-and-thrust belt. In broken foreland settings, deformation may be accommodated far into the foreland by reactivation of pre-existing crustal weaknesses, producing steep but short-wavelength topography within both the orogen and the foreland. The discontinuous nature of this deformation and potentially rapid rock uplift rates relative to those within fold-and-thrust belts favors sediment ponding behind active mountain ranges built atop old, reactivated geologic structures. Indeed, many sedimentary basins located within the headwaters of fluvial systems draining the margin of the Altiplano-Puna Plateau

show clear evidence of multiple episodes of filling as downstream ranges experience rock uplift accommodated along reactivated extensional structures. However, due to the proximity of these basins to mountain flanks with high precipitation and efficient headward erosion, these basins are often re-excavated and attain fluvial connectivity with the remainder of the foreland.

The limited along-strike extent of short-wavelength topography produced by uplift along old structures in the central Andean broken foreland system of northwestern Argentina produces spatially restricted accommodation space relative to that observed farther north in the Bolivian fold-and-thrust belt. Instead, flexural basins occur directly adjacent to individual ranges and are limited in spatial extent relative to the foredeep depozone of uninterrupted foreland basins. In addition, the limited flexural response to short-wavelength topographic loads may fail to create a well-defined forebulge or backbulge depozone. Thus, the application of existing foreland basin models to broken foreland basin systems is limited. These systems should be viewed in a context that considers their distinct deformation style and topography relative to typical foreland basin settings.

REFERENCES

- Allmendinger, R.W., Jordan, T.E., Kay, S.M. and Isacks, B.L. (1997) The evolution of the Altiplano-Puna Plateau of the central Andes. *Ann. Rev. Earth and Planet. Sci.*, 25, 139–174.
- Allmendinger, R.W., Ramos, V.A., Jordan, T.E., Palma, M. and Isacks, B.L. (1983) Paleogeography and Andean structural geometry, northwest Argentina. *Tectonics*, 2, 1–16.
- Alonso, R.N., Viramonte J, Gutierrez R. (1984) Puna Austral – Bases para el subprovincialismo geológico de la Puna Argentina. IX Congr. Geol. Arg. S. C. Bariloche. Actas 1, 43–63, Argentina.
- Alonso, R.N., Jordan, T.E., Tabbutt, K.T. and Vandervoort, D.S. (1991) Giant evaporite belts of the Neogene central Andes. *Geology*, 19, 401–404.
- Baby, P., Rochat, P., Mascle, G. and Héral, G. (1997) Neogene shortening contribution to crustal thickening in the back-arc of the Central Andes. *Geology*, 25, 883–886.
- Barazangi, M. and Isacks, B.L. (1976) Spatial distribution of earthquakes and subduction of the Nazca Plate beneath South America. *Geology*, 4, 686–692.
- Bevis, M. and Isacks, B.L. (1984) Hypocentral trend surface analysis: probing the geometry of Benioff Zones. *J. Geophys. Res.*, 89, 6153–6170.
- Bookhagen, B. and Strecker, M.R. (2008) High-resolution TRMM rainfall, hillslope angles, and relief along the eastern Andes. *Geophys. Res. Lett.*, 35, L06403, doi: 10.1029/2007GL032011.
- Bookhagen, B. and Strecker, M.R. (2010) Modern Andean rainfall variation during ENSO cycles and its impact on the Amazon drainage basin, in Hoorn, C. and Wesselink, F.P. *Amazonia, landscape and species evolution: a look into the past*. Oxford, Blackwell Publishing, 223–241.
- Bossi, G.E. and Palma, R.M. (1982) Reconsideración de la estratigrafía del Valle de Santa María, Provincia de Catamarca, Argentina. V. Congr. Latinoamericano Geol., Buenos Aires, Argentina, 155–172.
- Bossi, G.E., Georgieff, S.M., Gavrilloff, I.J.C., Ibañez, L.M., and Muruaga, C.M. (2001) Cenozoic evolution of the intramontane Santa María basin, Pampean Ranges, northwestern Argentina. *J. South Am. Earth Sci.*, 14, 725–734.
- Cahill, T. and Isacks, B.L. (1992) Seismicity and shape of the subducted Nazca plate. *J. Geophys. Res.*, 97, 17503–17529.
- Carrapa, B., Adelman, D., Hillel, G.E., Mortimer, E., Sobel, E.R., and Strecker, M.R. (2005) Oligocene uplift and development of plateau morphology in the southern central Andes. *Tectonics*, 24, 1–19, doi: 10.1029/2004TC001762.
- Carrapa, B., Hauer, J., Schoenbohm, L., Strecker, M.R., Schmitt, A., Villanueva, A., and Sosa Gomez, J. (2009) Dynamics of deformation and sedimentation in the northern Sierras Pampeanas: an integrated study of the Neogene Fiambalá basin, NW Argentina. *Bull. Geol. Soc. Am.*, 120, 1518–1543.
- Carrera, N., Muñoz, J.A., Sábat, F., Mon, R., and Roca, E. (2006) The role of inversion tectonics in the structure of the Cordillera Oriental (NW Argentinean Andes). *J. Structural Geology*, 28, 1921–1932.
- Coutand, I., Carrapa, B., Deeken, A., Schmitt, A.K., Sobel, E.R., Strecker, M.R. (2006) Orogenic plateau formation and lateral growth of compressional basins and ranges: insights from sandstone petrography and detrital apatite fission-track thermochronology in the Angastaco Basin, NW-Argentina. *Basin Research*, 18, 1–26.
- Crampton, S.L. and Allen, P.A. (1995) Recognition of forebulge unconformities associated with early stage foreland basin development: example from the North Alpine foreland basin. *Am. Assoc. Petrol. Geol. Bull.*, 79, 1495–1514.
- Cristallini, E., Comminguez, A., and Ramos, V.A. (1997) Deep structure of the Metán-Guachipas region: tectonic inversion in Northwestern Argentina. *J. South Am. Earth Sci.*, 10, 403–421.
- Cristallini, E., Comminguez, A., Ramos, V.A., and Mercerat, E.D. (2004) Basement double-wedge thrusting in the northern Sierras Pampeanas of Argentina (27° S) – constraints from deep seismic reflection, in K. R. McClay (editor) *Thrust tectonics and hydrocarbon systems*. Am. Assoc. Petrol. Geol. Memoir, 82, 65–90.
- Dahlen, F.A. (1984) Non-cohesive Critical Coulomb Wedges: an exact solution. *J. Geophys. Res.*, 89, 10125–10133.
- DeCelles, P.G. and Giles, K.A. (1996) Foreland basin systems. *Basin Research*, 8, 105–123.
- DeCelles, P.G. and Hertel, F. (1989) Petrology of fluvial sands from the Amazonian foreland basin, Peru and Bolivia. *Bull. Geol. Soc. Am.*, 101, 1552–1562.
- DeCelles, P.G. and Horton, B.K. (2003) Early to middle Tertiary foreland basin development and the history of Andean crustal shortening in Bolivia. *Bull. Geol. Soc. Am.*, 115, 58–77.
- de Urreiztieta, M., Gapais, D., LeCorre, C., Cobbold, P.R., and Rosello, E. (1996) Cenozoic dextral transpression

- and basin development at the southern edge of the Puna Plateau, northwestern Argentina. *Tectonophysics*, 254, 17–39.
- Dickinson, W.R. (1974) Plate tectonics and sedimentation. *Spec. Publ. SEPM*, 22, 1–27.
- Dickinson, W.R. and Snyder, W.S. (1978) Plate tectonics of the Laramide orogeny, in I. Matthews, V., ed., *Laramide folding associated with basement block faulting in the western United States*, Geol. Soc. America Memoir, 151. Denver, CO, Geol. Soc. America, 355–366.
- Dickinson, W.R. and Suczek, C.A. (1979) Plate tectonics and sandstone compositions. *Am. Assoc. Petrol. Geol. Bull.*, 63, 2164–2182.
- Echavarria, L., Hernandez, R., Allmendinger, R., and Reynolds, J. (2003) Subandean thrust and fold belt of northwestern Argentina: geometry and timing of the Andean evolution. *Am. Assoc. Petrol. Geol. Bull.*, 87, 965–985.
- Elger, K., Oncken, O. and Glodny, J. (2005) Plateau-style accumulation of deformation: southern Altiplano. *Tectonics*, 24, TC4020. doi: 10.1029/2004TC001675.
- Gephart, J.E. (1994) Topography and subduction geometry in the Central Andes: Clues to the mechanics of a non-collisional orogen. *J. Geophys. Res.*, 99, 12279–12288.
- González-Bonorino, F. (1950) Algunos problemas geológicos de las Sierras Pampeanas. *Rev. Asoc. Geol. Argent.*, 5, 81–110.
- Grier, M.E., Salfity, J.A. and Allmendinger, R.W. (1991) Andean reactivation of the Cretaceous Salta Rift, northwestern Argentina. *J. South Am. Earth Sci.*, 4, 351–372.
- Hain, M.P., Strecker, M.R., Bookhagen, B., Alonso, R.N., Pingel, H., and Schmitt, A.K. (2011) Neogene to Quaternary broken foreland formation and sedimentation dynamics in the Andes of NW Argentina (25°S). *Tectonics*, 30, TC2006. doi: 10.1029/2010TC002703.
- Hilley, G.E., Blisniuk, P.M. and Strecker, M.R. (2005) Mechanics and erosion of basement-cored uplift provinces. *J. Geophys. Res.*, 110 B12409. doi: 10.1029/2005JB003704.
- Hilley, G.E. and Coutand, I. (2010) Links between topography, erosion, rheological heterogeneity, and deformation in contractional settings: insights from the Central Andes. *Tectonophysics*, 95, 78–92.
- Hilley, G.E. and Strecker, M.R. (2005) Processes of oscillatory basin filling and excavation in a tectonically active orogen: Quebrada del Toro Basin, NW Argentina. *Bull. Geol. Soc. Am.*, 117, 887–901.
- Hongn, F., del Papa, C., Powell, J., Petrinovic, I., Mon, R., and Deraco, V. (2007) Middle Eocene deformation and sedimentation in the Puna-Eastern Cordillera transition (23–26°S): control by preexisting heterogeneities on the pattern of initial Andean shortening. *Geology*, 35, 271–274.
- Horton, B.K. and DeCelles, P.G. (1997) The modern foreland basin system adjacent to the Central Andes. *Geology*, 25, 895–898.
- Horton, B.K. and DeCelles, P.G. (2001) Modern and ancient fluvial megafans in the foreland basin system of the central Andes, southern Bolivia: implications for drainage network evolution in fold-thrust belts. *Basin Research*, 13, 43–63.
- Horton, B.K., Hampton, B.A., LaReau, N. and Baldellón, E. (2002) Tertiary provenance history of the northern and central Altiplano (central Andes, Bolivia): a detrital record of plateau-margin tectonics. *J. Sediment. Res.*, 72, 711–726.
- Iaffa, D.N., Sábat, F., Bello, D., Ferrer, O., Mon, R. and Gutierrez, A.A. (2011) Tectonic inversion in a segmented foreland basin from extensional to piggy back settings: the Tucumán basin in NW Argentina. *J. South Am. Earth Sci.*, 31, 457–474.
- Jacobi, R.D. (1981) Peripheral bulge: a causal mechanism for the Lower Ordovician unconformity along the western margin of the northern Appalachians. *Earth and Planetary Science Letters*, 56, 245–251.
- Jordan, T.E. (1981) Thrust loads and foreland basin evolution, Cretaceous, western United States. *Am. Assoc. Petrol. Geol. Bull.*, 65, 2506–2520.
- Jordan, T.E. (1995) Retroarc foreland and related basins, in C.J. Busby and R.V. Ingersoll, eds., *Tectonics of sedimentary basins*. Oxford, Blackwell Science, 331–362.
- Jordan, T.E. and Allmendinger, R.W. (1986) The Sierras Pampeanas of Argentina: a modern analogue of Rocky Mountain foreland deformation. *Am. J. Sci.*, 286, 737–764.
- Jordan, T.E. and Alonso, R.N. (1987) Cenozoic stratigraphy and basin tectonics of the Andes mountains, 20–28°S lat. *Am. Assoc. Petrol. Geol. Bull.*, 71, 49–64.
- Karner, G.D. and Watts, A.B. (1983) Gravity anomalies and flexure of the lithosphere at mountain ranges. *J. Geophys. Res.*, 88, 10449–10477.
- Kennan, L., Lamb, S. and Rundle, C. (1995) K-Ar dates from the Altiplano and Cordillera Oriental of Bolivia: implications for Cenozoic stratigraphy and tectonics. *J. South Am. Earth Sci.*, 8, 163–186.
- Kley, J. and Monaldi, C.R. (2002) Tectonic inversion of the Santa Barbara System of the central Andean foreland thrust belt, northwestern Argentina. *Tectonics*, 21, 1061–1072.
- Kley, J., Rosello, E.A., Monaldi, C.R., Habighorst, B. (2005) Seismic and field evidence for selective inversion of Cretaceous normal faults, Salta rift, northwest Argentina. *Tectonophysics*, 399, 155–172.
- Kraemer, B., Adelmann, D., Alten, M., Schnurr, W., Erpenstein, K., Kiefer, E., van den Bogaard, P., and Goerler, K. (1999) Incorporation of the Paleogene foreland into the Neogene Puna Plateau; the Salar de Antofalla area, NW Argentina. *J. South Am. Earth Sci.*, 12, 157–182.
- Marshak, S., Karlstrom, K., and Timmons, J.M. (2000) Inversion of Proterozoic extensional faults: an explanation for the pattern of Laramide and ancestral Rockies intracratonic deformation, United States. *Geology*, 28, 735–738.
- McQuarrie, N. (2002) The kinematic history of the central Andean fold-thrust belt, Bolivia: Implications for building a high plateau. *Bull. Geol. Soc. Am.*, 114, 950–963.
- Métivier, F., Y. Gaudemer, P. Tapponnier, and B. Meyer (1998) Northeastward growth of the Tibetan Plateau deduced from balanced reconstructions of two depositional areas: the Qaidam and Hexi corridor basins, China. *Tectonics*, 17, 823–842.
- Mitrovica, J.X., Beaumont, C. and Jarvis, G.T. (1989) Tilting of continental interiors by the dynamical effects of subduction. *Tectonics*, 8, 1079–1094.
- Mon, R., and Hongn, F. (1991) The structure of the Precambrian and lower Paleozoic basement of the central Andes between 22° and 32°S lat. *Geologische Rundschau*, 80, 745–758.

- Mon, R. and Salfit, J.A. (1995) Tectonic evolution of the Andes of northern Argentina, in Tankard, A.J., Suárez Soruco, R., Welsink, H.J., (editors) Petroleum basins of South America. Am. Assoc. Petrul. Geol. Memoir, 62, 269–83.
- Mora, A., Parra, M., Strecker, M.R., Kammer, A., Dimat, C. and Rodriguez, F. (2006) Cenozoic contractional reactivation of Mesozoic extensional structures in the Eastern Cordillera of Colombia. *Tectonics*, 25, TC2010, doi: 10.1029/2005TC001854.
- Mortimer, E., Carrapa, B., Coutand, I., Schoenbohm, L., Sobel, E.R., Sosa Gomez, J., and Strecker, M.R. (2007) Compartmentalization of a foreland basin in response to plateau growth and diachronous thrusting: El Cajón-Campo Arenal basin, NW Argentina. *Bull. Geol. Soc. Am.*, 119, 637–665.
- Parra, M., Mora, A., Jaramillo, C., Strecker, M.R., Sobel, E., Quiroz, L., Rueda, M., and Torres, V. (2009) Orogenic advance in the northern Andes: evidence from the oligocene sedimentary record of the Medina Basin, Eastern Cordillera, Colombia. *Bull. Geol. Soc. Am.*, 121, 780–800.
- Quinlan, G.M. and Beaumont, C. (1984) Appalachian thrusting, lithospheric flexure, and the Paleozoic stratigraphy of the Eastern Interior of North America. *Can. J. Earth Sci.*, 21, 973–996.
- Ramos, V.A., Cristallini, E.O., and Perez, E.J. (2002) The Pampean flat-slab of the Central Andes. *J. South Am. Earth Sci.*, 15, 59–78.
- Ramos, V. A., R. N. Alonso, and M. R. Strecker (2006) Estructura Y Neotectónica de la Lomas de Olmedo, Zona de transición entre los sistemas Subandino y de Santa Bárbara Provincia de Salta. Asoc. Geol. Argent. Rev., 4, 579–588.
- Reynolds, J. H., Galli, C. I., Hernández, R. M., Idleman, B. D., Kotila, J. M., Hilliard, R. V., and Naeser, C. W. (2000) Middle Miocene tectonic development of the Transition Zone, Salta Province, northwest Argentina: magnetic stratigraphy from the Metán Subgroup, Sierra de González. *Bull. Geol. Soc. Am.*, 112, 1736–1751.
- Reynolds, J.H., Hernandez, R.M., Galli, C.I., and Idleman, B.D. (2001) Magnetostriatigraphy of the Quebrada La Porcelana section, Sierra de Ramos, Salta Province, Argentina: age limits for the Neogene Orán Group and uplift of the southern Sierras Subandinas. *J. South Am. Earth Sci.*, 14, 681–692.
- Riller, U., Petrinovic, I., Ramešov, J., Strecker, M., and Oncken, O. (2001) Late Cenozoic tectonism, caldera and plateau formation in the central Andes. *Earth and Planetary Science Letters*, 188, 299–311.
- Schwab, F.L. (1986) Sedimentary "signatures" of foreland basin assemblages: real or counterfeit, in Allen, P.A., and Homewood, P., eds., *Foreland Basins*. Spec. Publ. Int. Assoc. Sed. 395–410.
- Sempere, T., Herail, G., Oller, J., and Bonhomme, M.G. (1990) Late Oligocene-Early Miocene major tectonic crisis and related basins in Bolivia. *Geology*, 18, 946–949.
- Sobel, E.R., Hilly, G.E. and Strecker, M.R. (2003) Formation of internally drained contractional basins by aridity-limited bedrock incision. *J. Geophys. Res.*, 108, (B7) 2344, doi: 10.1029/2002JB001883.
- Sobel, E.R. and Strecker, M.R. (2003) Uplift, exhumation and precipitation: tectonic and climatic control of Late Cenozoic landscape evolution in the northern Sierras Pampeanas, Argentina. *Basin Research*, 15, 431–451.
- Starck, D., and Anzótegui, L.M. (2001) The late Miocene climatic change—Persistence of a climatic signal through the orogenic stratigraphic record in northwestern Argentina. *J. South Am. Earth Sci.*, 14, 763–774.
- Steidmann, J.R., McGee, L.C., and Middleton, L.T. (1983) Laramide sedimentation, folding, and faulting in the southern Wind River Range, Wyoming, in Lowell, J.D., ed., *Rocky Mountain foreland basins and uplifts*. Rocky Mountain Association of Geologists, Denver, 161–167.
- Stenzlauer, A. (1923) Contribución a la geología de la República Argentina, con la parte límitrofe de los Andes Chilenos entre los 32° y 33° S. *Actas Acad. Nac. Cienc. Córdoba, Argentina* 8, 1–28.
- Stecker, M.R., Carvany, P., Bloom, A.L., and Malizia, D. (1989) Late Cenozoic tectonism and landscape development in the foreland of the Andes: Northern Sierras Pampeanas, Argentina. *Tectonics*, 8, 517–534.
- Strecker, M.R. and Marrett, R. (1999) Kinematic evolution of fault ramps and its role in development of landslides and lakes in the northwestern Argentine Andes. *Geology*, 27, 307–310.
- Strecker, M.R., Alonso, R.N., Bookhagen, B., Carrapa, B., Hillay, G.E., Sobel, E.R., and Trauth, M.H. (2007) Tectonics and climate of the Southern Central Andes. *Ann. Rev. Earth and Planet. Sci.*, 35, 747–787.
- Tassara, A., Swain, C., Hackney, R., and Kirby, J. (2007) Elastic thickness structure of South America estimated using wavelets and satellite-derived gravity data. *Earth and Planetary Science Letters*, 253, 17–36.
- Trauth, M.H., Alonso, R.N., Haselton, K., Hermanns, R.L., and Strecker, M.R. (2000) Climate change and mass movements in the northwest Argentine Andes: Earth and Planetary Science Letters, 179, 243–256.
- Turcotte, D.L. and Schubert, G. (2002) *Geodynamics*. Cambridge University Press, Cambridge, England, 456 pp.
- Uba, C.E., Hulk, C., and Heubeck, C. (2006) Evolution of the late Cenozoic Chaco foreland basin, Southern Bolivia. *Basin Research*, 18, 145–170.
- Vandervoort, D.S., Jordán, T.E., Zaitler, P.K., and Alonso, R. (1995) Chronology of internal drainage development and uplift, southern Puna plateau, Argentine central Andes. *Ceology*, 23, 145–148.
- Wara, M.W., Ravelo, A.C., and Delaney, M.L. (2005) Permanent El Niño-like conditions during the Pliocene warm period. *Science*, 309, 758–761.
- Wilkinson, M.J., Marshall, L.G., Lundberg, J.G., and Krasil'sky, M.H. (2010) Megafan environments in northern South America and their impact on Amazon Neogene aquatic ecosystems, in Hoorn, C. and Wesselingh, F.P., eds., *Amazonia, landscape and species evolution: a look into the past*. Oxford, Blackwell Publishing, 162–184.